Desalination and Water Treatment
www.deswater.com

doi: 10.1080/19443994.2016.1144534

57 (2016) 25194–25206
November

Taylor & Francis
Taylor & Francis Group

Adsorption of methylene blue onto activated carbon developed from biomass waste by H_2SO_4 activation: kinetic, equilibrium and thermodynamic studies

Ali H. Jawad[a,b,*], Ramlah Abd Rashid[a], Mohd Azlan Mohd Ishak[a,b], Lee D. Wilson[c]

[a]*Faculty of Applied Sciences, Coal and Biomass Energy Research Group, Universiti Teknologi MARA, Arau Campus, Arau, Perlis 02600, Malaysia, Tel. +60 49882571; emails: ahjm72@yahoo.com, ahjm72@gmail.com (A.H. Jawad), Tel. +60 124872038; email: d_chemist@yahoo.com (R.A. Rashid), Tel. +60 49882027; email: azlanishak@perlis.uitm.edu.my (M.A.M. Ishak)*
[b]*Faculty of Applied Sciences, Universiti Teknologi MARA, Shah Alam, Selangor 40450, Malaysia*
[c]*Department of Chemistry, University of Saskatchewan, 110 Science Place, Saskatoon, Saskatchewan S7 N 5C9, Canada, Tel. +1 3067166405; email: lee.wilson@usask.ca*

Received 24 September 2015; Accepted 17 January 2016

ABSTRACT

Sulphuric acid (H_2SO_4) was utilized as an activator for the preparation of activated carbon from a biomass solid waste, coconut leaves. The sulphuric acid-treated activated carbon (SAC) was used as low-cost adsorbent for the removal of methylene blue (MB) cationic dye from aqueous solution. Adsorption of MB using SAC from aqueous solution under equilibrium and kinetic conditions in batch mode was evaluated by varying adsorbent dose (0.2–2.5 g/L), solution pH (3–11), initial dye concentration (30–400 mg/L), contact time (0–180 min) and temperature (303–323 K). The Langmuir isotherm model showed better fit to the equilibrium data than the Freundlich model. The adsorption capacity (q_m) of SAC increased with temperature where q_m varied as follows: 126.9 (303 K), 137.0 (313 K) and 149.3 mg/g (323 K). The kinetic uptake results were well described by the pseudo-second-order (PSO) kinetic for each temperatures. The thermodynamic adsorption parameters (ΔG°, ΔH° and ΔS°) were driven by favourable entropic factors, in accordance with the low activation energy (29.70 kJ/mol) of the system. This study reveals that SAC is an effective and low-cost adsorbent for the removal of MB from aqueous solution.

Keywords: Activated carbon; Adsorption; Coconut leaves; Methylene blue; Sulphuric acid; Chemical activation

1. Introduction

Wastewater pollution by various industrial activities has become a worldwide problem nowadays since uncontrolled release of pollutants presents a serious problem in aquatic environments due to acute and chronic toxicity to aquatic organisms, accumulation in the ecosystems, loss of habitats and biodiversity and human health risks [1]. Dyes and pigments present in wastewater result in aesthetic colouration even after minor release into the environment which causes concern for public health and environmental authorities. There are more than 100,000 commercial dyes that exist with more than 7×10^5 t produced annually [2]. Basic dyes are cationic dyes with electronic characteristics that originate from positively charged nitrogen or sulphur atoms in dye structure. Basic dyes present

*Corresponding author.

an obvious colouration even at low concentration (<1 mg/L) and have been classified as toxic colourants [3]. Methylene blue (MB) is a basic (cationic) dye, which is water soluble with industrial applications as a dyeing agent for leather, calico, cotton and tannins, in addition to use as a biological staining agent [4]. The acute exposure to MB dye causes eye and gastrointestinal problems according to symptoms of irritation, nausea, vomiting and diarrhoea. MB dye exposure may also result in methaemoglobinaemia, cyanosis, convulsions and dyspnoea [5].

Many treatment methods for the removal of dyes from industrial effluents include adsorption [6], bioremediation [7], electrochemical degradation [8], cation exchange membranes [9], Fenton chemical oxidation [10], photocatalytic degradation [11,12] and flocculation–coagulation [13]. Among the various methods, adsorption is one of the most effective treatment techniques for advanced wastewater treatment to reduce hazardous waste pollutants in effluent. Adsorption-based treatment with appropriate adsorbent materials displays high performance and selectivity, flexibility and simplicity of design, convenience of operation without producing harmful by-products [3–6].

Activated carbon (AC) is a widely used industrial carbonaceous adsorbent due to its high surface area, variable pore structure, high adsorption capacity and occurrence of various surface functional groups, according to the mode of preparation. Carbonaceous solid precursors from natural or synthetic sources can be used to produce activated carbon [14]. Research and development of carbonaceous adsorbents from agricultural waste is an area of ongoing interest because the precursors are cheap, renewable, safe and abundant. Besides AC, there are unconventional biomass precursors that had been developed as effective adsorbents such as indigenous acclimated mixed culture [15], *Setaria verticillata* grasses [16], and poly sulpha sponge [17] for dye removal and pharmaceutical wastewater treatment.

Coconut (*Cocos nucifera*) is a versatile palm tree that belongs to the Arecaceae family. The palm tree grows well under warm and humid conditions and is commonly found in tropical and sub-tropical regions. Coconut has been widely used as a source of food, fuel, drink, edible oil, fibre, animal feed and building materials. In Malaysia, coconut is the fourth most important industrial crop [18] which results in large amounts of coconut waste, where waste disposal remains a serious environmental problem. Coconut leaf biomass has limited use and economic value. The waste disposal can be addressed by valorization of these low-cost by-products by conversion into AC. The development of coconut leaf-based AC would address the issues of waste disposal and offer an inexpensive precursor alternative for production.

The adsorption properties of AC strongly depend on the nature and preparation of the source materials including the activation steps, such as physical (thermal) or chemical activation. Physical activation is a two-step process where conversion of the precursor into carbonized material (char) is followed by activation with an oxidizing gas such as carbon dioxide, water vapour or their mixtures [19]. In chemical activation, the precursor is impregnated with dehydrating chemical agents including phosphoric acid (H_3PO_4), sulphuric acid (H_2SO_4) and zinc chloride ($ZnCl_2$), and carbonization at variable temperatures [20]. Chemical activation has some advantages since it employs lower temperatures and has higher carbonization yield than physical activation [21].

Among the various types of chemical activation agents, sulphuric acid is frequently used for the preparation of carbon adsorbents from lignocellulose products. H_2SO_4 gives the possibility to develop porous structure by degrading the amorphous domains of cellulosic materials of plant materials and the aromatization of the carbon framework [22]. H_2SO_4 has been frequently used as an activation agent to produce AC from different biomass sources such as bagasse [4], *Euphorbia rigida* [22], almond husk [23], agricultural waste (*Parthenium hysterophorus*) [24], sunflower and oil cake [25], pine fruit shell [26], *Delonix regia* pods [27], potato peel and neem bark [28]. Therefore, the key objectives of this study was to develop a low-cost AC adsorbent from coconut leaves with H_2SO_4 activation. The adsorption properties of the sulphuric acid-activated AC (SAC) were studied with MB in aqueous solution under equilibrium and kinetic conditions to obtain the associated adsorption parameters. To the best of our knowledge, this work is the first reported example of the use of coconut leaves as a precursor for preparing AC via chemical activation with H_2SO_4.

2. Materials and methods

2.1. Preparation and characterization of SAC

The coconut leaf powder was prepared according to the method reported by Jawad et al. [6] and the process for H_2SO_4 activation was adopted according to the method reported by Garg et al. [29]. The SAC product was ground and sieved to obtain a powder with a particle size range of 150–212 μm. The yield of SAC was calculated according to a published method [30] and the bulk or apparent density was determined by following the method reported by Ahmedna et al. [31]. The moisture content was determined by an oven

drying method [32], where the ash content determination used standard methods [33]. The iodine number is a measure of micropore content (0–20Å) and was obtained by a standard method [34]. The proximate analysis of the SAC was performed using a muffle furnace and the elemental analysis was carried out using a CHN analyzer (Perkin-Elmer, Series II, 2400). The pH at the *point-of-zero* charge (pH_{PZC}) was estimated using a pH meter (Metrohm, Model 827 pH Lab, Switzerland), as described elsewhere [35]. The functional groups of SAC before and after MB adsorption were measured by Fourier transform infrared (FTIR) spectroscopy (PerkinElmer, Spectrum RX I), with a spectral range from 4,000 to 400 cm^{-1}. The surface morphology of SAC before and after adsorption of MB was measured using a scanning electron microscope (SEM; SEM-EDX, FESEM CARL ZEISS, SUPKA 40 VP).

2.2. Adsorbate (MB)

Methylene blue (MB) was purchased from R&M Chemicals (CI 52015) with a chemical formula ($C_{16}H_{18}ClN_3S{\cdot}xH_2O$) and molecular weight (319.86 g/mol).

2.3. Batch adsorption experiments

The batch adsorption experiments of MB onto SAC were performed in a series of 250-mL Erlenmeyer flasks containing 200 mL of MB solution. The flasks were capped and agitated in an isothermal water bath shaker (Memmert, waterbath, model WNB7-45, Germany) at fixed shaking speed of 110 rpm and 303 K until equilibrium was attained. Batch adsorption experiments were carried out by varying several experimental variables such as adsorbent dosage (0.5–2.5 g/L), pH (3–11), initial dye concentration (30–400 mg/L) and contact time (0–180 min) to determine the optimum uptake conditions for adsorption. The pH of MB solution was adjusted by adding either 0.10 M HCl or NaOH. After mixing of the SAC–MB system, the supernatant was collected with a 0.20-μm Nylon syringe filter and the concentrations of MB were monitored at a different time interval using a HACH DR 2800 Direct Reading Spectrophotometer at the maximum wavelength (λ_{max}) of absorption at 661 nm. For the thermodynamic studies, similar procedures were applied at 313 and 323 K, with the other variables held constant. The adsorption capacity at equilibrium, q_e (mg/g) and the per cent of colour removal, CR (%) of MB were calculated using Eqs. (1) and (2).

$$q_e = \frac{(C_0 - C_e)V}{W} \quad (1)$$

$$CR\% = \frac{(C_0 - C_e)}{C_0} \times 100 \quad (2)$$

where C_0 is the initial dye concentration (mg/L); C_e is the dye concentration at equilibrium (mg/L); V is the volume of dye solution (mL); and W is the dry mass of the adsorbent (g). Adsorption experiments were conducted in triplicate under identical conditions and the results are reported as an average value.

3. Results and discussion

3.1. Characterization of SAC

3.1.1. Physical properties

The results of physical characterization of SAC are outlined in Table 1. The results indicate that SAC has a moderate iodine number, low values of bulk density, ash content and moisture content, along with a relatively high yield of carbon.

3.1.2. FTIR spectral analysis

The pattern of adsorption onto biomass materials is related to the availability of active functional groups and bonds of the AC surface. For the elucidation of these active sites, FTIR spectral analysis was performed. Several IR bands appearing in the FTIR spectrum of SAC before adsorption (Fig. 1(a)) that were assigned to various functional groups, in accordance with their respective wavenumber (cm^{-1}) position as

Table 1
Physicochemical characteristics of the activated carbon (SAC)

Typical properties	
Bulk density (g/mL)	0.58
Iodine number (mg/g)	263
Proximate analysis (wt.%)	
Ash content	7.90
Moisture content	16.23
Fixed carbon (yield)	63.68
Volatile matter	12.19
Ultimate analysis (wt.%)	
C	75.09
H	4.96
N	0.81
S	0.39
O (by difference)	18.75

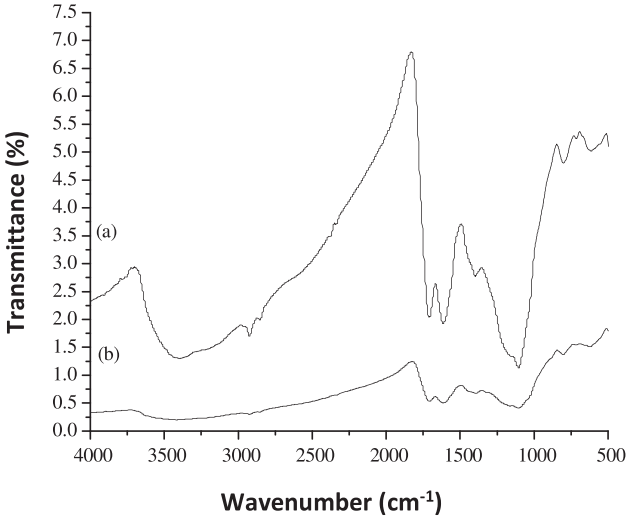

Fig. 1. FT-IR spectra of SAC (a) before MB adsorption and (b) after MB adsorption.

reported in the literature. The region between 3,600 and 2,600 cm^{-1} indicates two major IR bands, where a broad and strong band stretch is observed from 3,600 to 3,000 cm^{-1}. The latter indicates the presence of free or hydrogen-bonded O–H groups (alcohols, carboxylic acids and phenols) as in pectin, cellulose and lignin on the surface of the adsorbent [36]. The O–H stretching vibrations occur within a broad range of frequencies indicating the presence of "free" hydroxyl groups and bonded O–H bands such as carboxylic acids. The weak band observed from 2,900 to 2,750 cm^{-1} is assigned to the aliphatic C–H stretching (methine, methyl and methylene groups of side chains) and from aromatic C–H stretching near 3,100 cm^{-1}. The band at about 1,700 cm^{-1} relates to C=O stretching of ketones, aldehydes, lactones or carboxyl groups, and the band at 1,600–1,580 cm^{-1} is assigned to C=C vibrations in aromatic rings [37]. The IR band at ca. 1,400 cm^{-1} to 1,300 cm^{-1} relates to the asymmetric stretching of the sulphonic acid groups ($-SO_3$) [38]. The IR bands between 1,300 and 1,000 cm^{-1} are observed for oxidized carbon materials and are assigned to C–O and/or C–O–C stretching in acids, alcohols, phenols, ethers and/or esters groups and sulphonic acid groups ($-SO_3$). The shoulders between 900 cm^{-1} and 800 cm^{-1} were ascribed to the stretching of the S=O bond, according to Liang et al. [39]. Thus, the FTIR spectrum of SAC before adsorption (Fig. 1(a)) indicates that the external surface of SAC is rich in functional groups, containing oxygen of carboxylic, carbonyl and phenolic species. After adsorption of MB, the spectrum of SAC (Fig. 1(b)) shows attenuated band intensity where the functional groups either shifted in frequency or disappear in some cases when MB molecules are bound onto the SAC surface. These spectral changes in Fig. 1(b) indicate the possible involvement of those functional groups on the surface of SAC in the adsorption process.

3.1.3. pH_{PZC} of the SAC

Fig. 2 shows the pH_{PZC} results of the experiments performed with the SAC adsorbent, where the pH ranged from 2 to 12. According to Fig. 2, the pH_{pzc} of the SCA was 3.20, which indicates the acid character of the SAC surface, in agreement with the presence of acid groups from the IR results above (Fig. 1). Below the pH_{PZC} value, the surface of SAC is positively charged due to protonation, favouring the adsorption of anions. Above the pH_{PZC}, the SAC surface has a negative charge which favours the adsorption of cation species [38]. In this respect, Karagöz et al. [25] reported that the pH_{PZC} value lies between pH 2.5 and 5.5 which was attributed to the acid form of AC derived from sunflower oil cake treated with H_2SO_4.

3.1.4. Surface morphology of SAC

The surface morphology of SAC adsorbent was evaluated according to the SEM images obtained in Fig. 3. There is a change in surface morphology of the SAC powder before (Fig. 3(a)) and after the adsorption (Fig. 3(b)) of MB. According to Fig. 3(a), the surface features of SAC are rough and irregular along with heterogeneous cavities that well distributed across the SAC surface. Thus, the SEM images reveal that MB

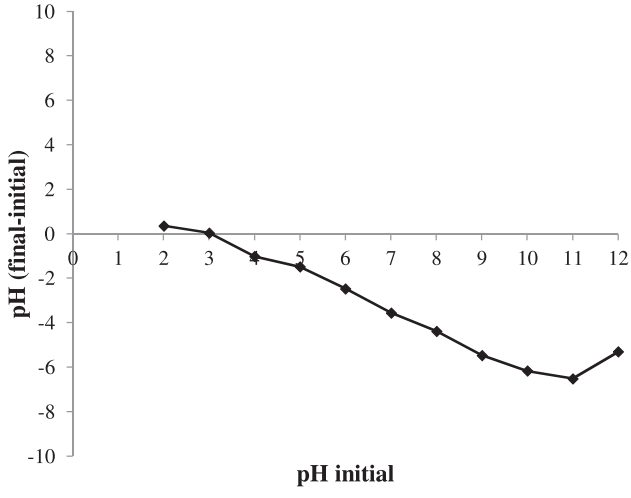

Fig. 2. pH_{PZC} of SAC suspensions.

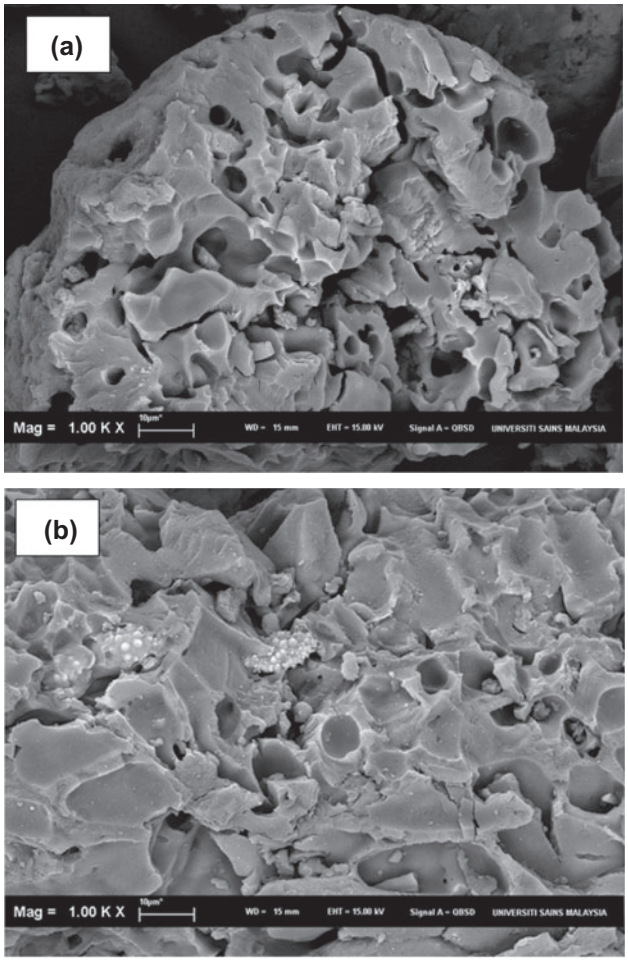

Fig. 3. Typical SEM micrograph of SAC particle (1,000 magnification): (a) before MB adsorption and (b) after MB adsorption.

may be adsorbed onto the SAC surface and the accessible pore domains of the carbonaceous surface. The surface morphology of SAC after MB adsorption reveals a change in the topography of the adsorbent, as evidenced by the appearance of reduced pore structure and smoother surface features due to the adsorption of MB in Fig. 3(b). There is some evidence in Fig. 3(b) that indicates localized concentration of bound MB and this may be related to the heterogeneous distribution of polar functional groups (e.g. −COOH, −OH, −NH, etc.) on the surface of SAC.

3.2. MB Adsorption

3.2.1. Effect of the adsorbent dosage

The effect of adsorbent dosage on the removal of the MB from aqueous solution was determined using variable quantities of SAC adsorbent ranging from 0.020 to 0.25 g at fixed volumes (100 mL) and initial dye solution where C_0 was 100 mg/L. For these tests, other operation parameters were held constant at 303 K, shaking speed of 110 rpm, contact time of 60 min and an unadjusted pH at 5.60 for the initial MB solution. The results are shown in Fig. 4. The highest level of MB removal was achieved using 0.15 g SAC. At elevated levels of SAC, the amount of MB removal remained almost constant. The observed increase in the dye removal (%) with adsorbent dose was attributed to an increase in the available adsorbent surface area, as the number of adsorption sites increase correspondingly [24,26,38]. These results indicate that the adsorbent dosage of SAC must be fixed at 0.15 g, corresponding to the minimum amount of adsorbent for effective MB removal. Hereafter, 0.15 g/100 mL was selected as an optimum SAC dosage for adsorption studies reported in this work.

3.2.2. Effect of pH

The pH of the solution influences the speciation of the dye, along with the surface charge of the adsorbent. The effect of initial pH on MB removal was carried out over the pH range 3–11 as shown in Fig. 5. The removal of MB increased remarkably as the pH of the solution increased from 3 up to 6. Moreover, no obvious change in MB removal was seen by increasing in the pH values to higher levels (pH 6–11). The lower adsorption of MB at acidic pH was accounted for by the competition at adsorption sites between the MB cations and excess H^+ ions in solution. At higher pH values, the surface of SAC adopts a negative surface charge, which contributes to enhanced uptake of positively charged dye species via attractive electrostatic attraction, in accordance with an increase in the rate of adsorption [40]. Moreover, the surface of the adsorbent

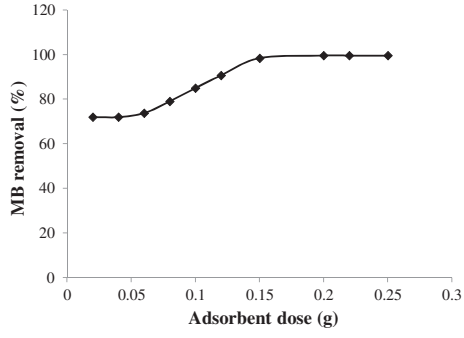

Fig. 4. Effect of SAC dosage on MB removal (%) at $[MB]_o$ = 100 mg/L, V = 100 mL, unadjusted pH 5.60, T = 303 K, shaking speed = 110 rpm and contact time = 60 min.

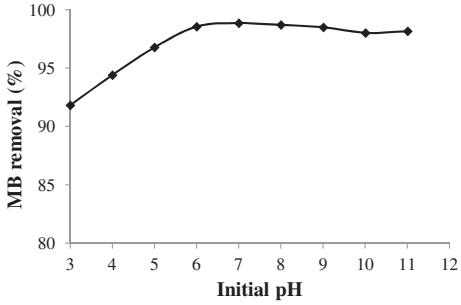

Fig. 5. Effect of pH on MB removal (%) using 0.15 g of SAC, $[MB]_o$ = 100 mg/L, V = 100 mL, T = 303 K, shaking speed = 110 rpm and contact time = 60 min.

was positively charged, since the pH was below the PZC, where pH_{PZC} = 3.20, contributing to electrostatic repulsion of MB cations at the SAC surface. This observation supports the results obtained from previous study of the pH_{PZC} reported by Royer et al. [26] for the removal of MB from aqueous solution using H_2SO_4-treated pine fruit shell adsorbent material. To continue this work, the effective pH for SAC was fixed at 6, and used in further adsorption studies herein.

3.2.3. Effect of initial dye concentration and contact time

The experimental results for the adsorption properties of MB onto SAC at various initial concentrations are shown in Fig. 6. The amount of MB adsorbed by the SAC adsorbent at equilibrium increased rapidly from 20.2 to 129 mg/g as the initial dye concentration increased from 30 to 400 mg/L. The effect can be attributed to the greater rate of collision rate between MB and SAC surface at higher initial dye concentration. Hence, additional amounts of MB were transferred to the SAC surface. Additional time was needed to reach equilibrium for higher dye concentration because there was a tendency for MB to penetrate deeper within the interior surface of the SAC and be adsorbed at active pore sites. This indicates that the initial dye concentration plays a significant role in the adsorption capacity of MB onto SAC sorbent. Similar observations were reported for the adsorption of MB on the surface of various AC materials obtained from different biomass sources prepared using H_2SO_4 activation [22,24,26].

3.2.4. Effect of temperature on dye adsorption

Temperature is anticipated to have an influence on the dye adsorption properties of SAC adsorbent with MB. The temperature effect on the adsorption capacity of SAC was tested at 303, 313 and 323 K with varying initial concentrations of 30–400 mg/L, as shown in Fig. 7. Accordingly, the observed equilibrium uptake properties increase with increasing temperature at all MB concentrations studied. The adsorption capacity of the SAC increased from 127.0 to 149.2 mg/g as the temperature increased from 303 to 323 K, as listed in Table 2. The observed results in Fig. 7 indicates that the adsorption process of MB onto SAC was favoured at higher temperature, in agreement with an endothermic adsorption process. This can be partly attributed to strong attractive forces between methylene blue and activated carbon at higher temperatures [41], along with the contributions due to desolvation of the SAC surface. The endothermic nature of adsorption was similarly reported for removal of MB from aqueous solution using H_2SO_4-treated bagasse [4], and *Euphorbia rigida* [22].

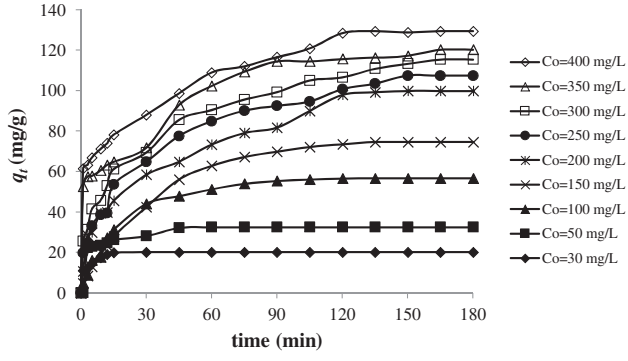

Fig. 6. Effect of contact time and initial concentration on the adsorption of MB by SAC (V = 200 mL, T = 303 K, shaking speed = 110 rpm and SAC mass = 0.30 g).

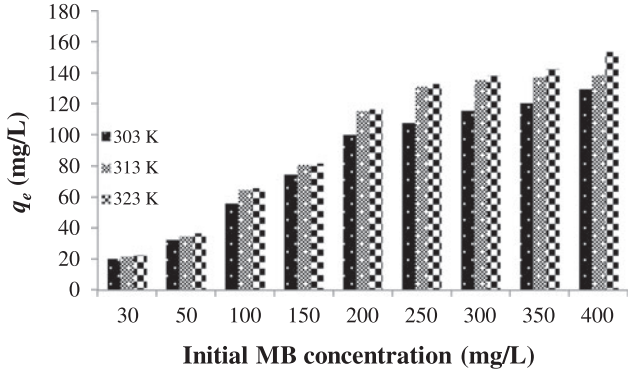

Fig. 7. Effect of temperature on the equilibrium adsorption capacity of SAC at different initial MB concentrations.

Table 2
Isotherm parameters for removal of MB by SAC at variable temperatures

	Langmuir isotherm		
Temperature (K)	q_m (mg/g)	K_L (L/mg)	R^2
303	126.6	0.137	0.991
313	137.0	0.226	0.999
323	149.3	0.312	0.992
	Freundlich isotherm		
Temperature (K)	K_F (mg/g (L/mg)$^{1/n}$)	$1/n$	R^2
303	41.7	0.210	0.987
313	51.6	0.214	0.978
323	61.8	0.155	0.915

3.3. Adsorption isotherm

The adsorption isotherm results for SAC were fitted using two types of commonly encountered isotherm models to evaluate a suitable model for describing the adsorption process. The Langmuir isotherm [42] is based on an assumption involving adsorption at homogeneous sites on surface of the adsorbent. As well, monolayer adsorption occurs onto a surface containing a finite number of adsorption sites with uniform adsorption and no transmigration of adsorbate on an idealized planar surface. The linearized form of the Langmuir isotherm is shown by Eq. (3):

$$\frac{C_e}{q_e} = \frac{1}{q_m K_L} + \frac{1}{q_m} C_e \quad (3)$$

where C_e is the equilibrium concentration (mg/L) and q_e is the amount of adsorbed species per specified amount of adsorbent (mg/g), K_L is the Langmuir equilibrium constant and q_m is the amount of adsorbate required to form an adsorbed monolayer. Hence, a plot of C_e/q_e vs. C_e should be a straight line with a slope ($1/q_m$) and an intercept ($1/q_m K_L$) as shown in Fig. 8.

By contrast, the Freundlich isotherm assumes heterogeneous surface energies, as described by a form of the Langmuir equation that varies as a function of the surface coverage [43]. The well-known linear form of Freundlich isotherm [44] is given by Eq. (4):

$$\ln q_e = \ln K_F + \frac{1}{n} \ln C_e \quad (4)$$

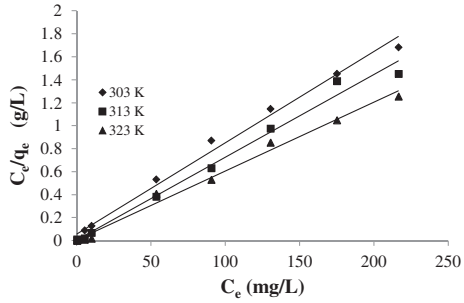

Fig. 8. Langmuir isotherm plots for the adsorption of MB onto SAC at variable temperatures.

where C_e is the equilibrium concentration of the adsorbate (mg/L), q_e is the amount of adsorbate adsorbed per unit mass of adsorbent (mg/g), K_F and n are the Freundlich constants where n indicates the relative favourability of the adsorption process. The affinity constant, K_F (mg/g (l/mg)$^{1/n}$, relates to the adsorption capacity of the adsorbent which can also be defined as the adsorption or distribution coefficient, and represents the quantity of dye adsorbed onto activated carbon for a unit equilibrium concentration. The plot of ln q_e vs. ln C_e (Fig. 9) yields a straight line with slope of $1/n$, whereas K_F was calculated from the intercept value.

The adsorption parameters for the two models at variable temperatures (303, 313 and 323 K) are listed in Table 2. The Langmuir model showed the best-fit results overall at each temperature, as evidenced by the greater R^2 values as compared with the Freundlich model. The essential characteristics of Langmuir isotherm can be expressed by a dimensionless separation factor (R_L) [45], defined by Eq. (5):

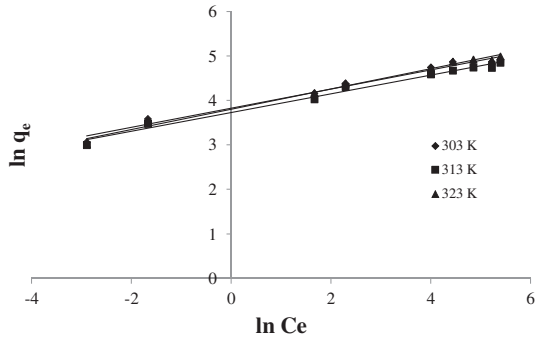

Fig. 9. Freundlich isotherm plots for the adsorption of MB onto SAC at variable temperatures.

$$R_L = \frac{1}{1 + K_L C_0} \tag{5}$$

An adsorption system is considered favourable when $0 < R_L < 1$, unfavourable when $R_L > 1$, linear when $R_L = 1$ or irreversible when $R_L = 0$. In this study, the values of R_L obtained were between 0 and 1 and indicate that the adsorption process is favourable for the SAC–MB system. The calculated R_L values at different initial MB concentrations are shown in Fig. 10. The values of R_L vary within the range of 0–1 for all initial concentrations of MB, and confirm the favourable adsorption of MB that occurs over the range of dye concentration and temperature values. According to the Freundlich isotherm model, the slope of $1/n$ ranges between 0 and 1, and is a measure of adsorption intensity or surface heterogeneity, becoming more heterogeneous as $1/n$ approaches zero. A value for $1/n$ below unity indicates a normal Langmuir isotherm, while $1/n$ above unity indicates cooperative adsorption [46]. Subsequently, the $1/n$ values obtained for SAC at three temperatures studied lie below unity. This revealed that the adsorption process followed a normal Langmuir isotherm profile. These results indicate that the surface binding sites of SAC are homogeneous nature where each dye is bound with similar adsorption energy [3]. The results reveal that the formation of a surface monolayer of dye molecules occurs for SAC, where the monolayer adsorption capacity (q_m) for SAC with MB was compared with other types of H_2SO_4-treated AC adsorbents in Table 3.

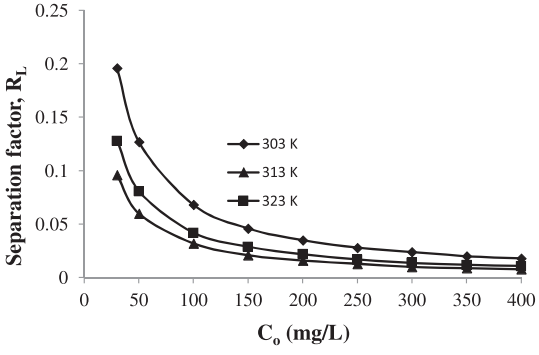

Fig. 10. Relation between initial MB concentration and the separation factor, R_L, for the adsorption of MB dye onto SAC at variable temperatures.

3.4. Adsorption kinetics

The rate and mechanism of the adsorption process was evaluated using three different kinetic models, namely pseudo-first-order model (PFO), pseudo-second-order model (PSO) and intraparticle diffusion model. The PFO was originally proposed by Lagergren [49] and its linearized form is given by Eq. (6):

$$\ln(q_e - q) = \ln(q_e) - (k_1)t \tag{6}$$

The amount of MB adsorbed by SAC at equilibrium [q_e (mg/g)] and time t [q_t (mg/g)], while k_1 (1/min) is the PFO rate constant. The values of k_1 were determined from the slope of the plots of $\ln(q_e - q_t)$ vs. t (Fig. 11(a)) where the values are given in Table 4. The linear form of the PSO model is given by Eq. (7) [50]:

$$\frac{t}{q_t} = \frac{1}{k_2 q_e^2} + \frac{t}{q_e} \tag{7}$$

The PSO rate constant (k_2; g/mg min) and $q_{e,cal}$ were calculated from the intercept and slope of t/q_t vs. t, shown in Fig. 11(b). The kinetic adsorption results of MB by SAC under various conditions were calculated from the related plots and the results are listed in Table 4. The correlation coefficients for the PSO kinetic model were higher than those for the PFO model. An increase in the temperature reveals an increase in the value of q_{cal}. In Table 4, the observed R^2 values are nearly unity ($R^2 \geq 0.99$) for the PSO kinetic model, where the values of $q_{e,cal}$ are in good agreement with $q_{e,exp}$. The PSO model provides insight about the possible rate-limiting step that controls the adsorption of MB onto AC obtained from H_2SO_4-treated bagasse [4], *Euphorbia rigida* [22] and sunflower oil cake [25], also potato peels and neem bark [28]. The PFO and PSO kinetic models describe the uptake behaviour of MB over the whole adsorption process; however, these models do not account for the diffusion mechanism.

Table 3
Comparison of adsorption capacities for MB onto different activated carbons prepared by H_2SO_4 activation

H_2SO_4-treated activated carbons	Adsorbent dosage, g	pH	Temperature (K)	q_{max} (mg/g)	Refs.
Coconut leaves	0.15 g/100 mL	6	303–323	127–149	This study
Almond husk	0.5 g/100 mL	5	293	37.2	[23]
Parthenium hysterophorus	0.4 g/100 mL	7	298	39.7	[24]
Euphorbia rigida	0.2 g/100 mL	6	293–313	114	[22]
Sunflower oil cake	0.2 g/100 mL	6	288–318	16.4	[25]
Neem bark	0.02 g/100 mL	2	298–318	5.71	[28]
Potato peel	0.02 g/100 mL	2	298–318	10.4	[28]
Delonix regia pods	0.1 g/50 mL	7	298	23.3	[27]
Pine fruit shell	0.06 g/20 mL	8.5	298	529	[26]
Ficus carica	0.5 g/100 mL	8	298–323	47.6	[47]
Coconut tree sawdust	0.5 g/100 mL	5	298	4.70	[48]
Silk cotton hull	0.5 g/100 mL	5	298	2.40	[48]
Sago waste	0.5 g/100 mL	5	298	4.51	[48]
Maize cob	0.5 g/100 mL	5	298	5.0	[48]
Banana pitch	0.5 g/100 mL	5	298	4.67	[48]
Bagasse	0.4 g/100 mL	9	300–333	49.8–56.5	[4]

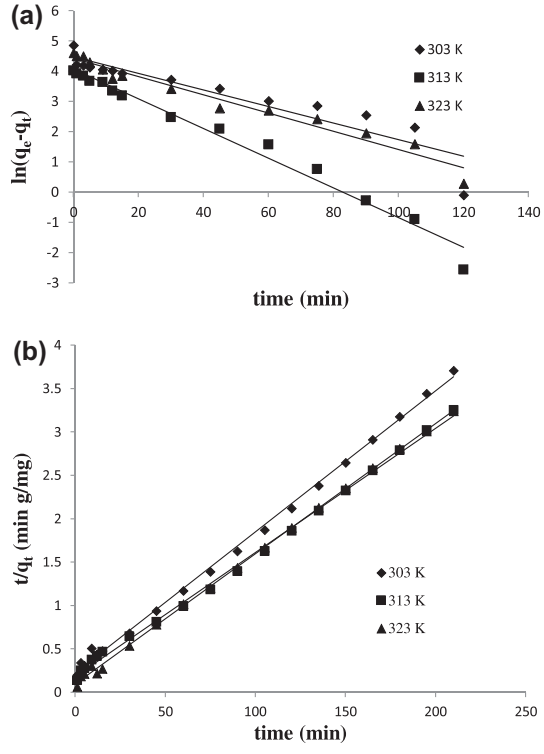

Fig. 11. Kinetic profiles for the adsorption of MB onto SAC at variable temperatures: (a) PFO and (b) PSO.

Table 4
Comparison of the pseudo-first-order (PFO), pseudo-second-order (PSO) and intraparticle diffusion models for the adsorption of MB on SAC at variable temperatures

	Temperature (K)		
	303	313	323
q_{exp}	56.7	64.6	64.8
PFO			
q_{cal}	87.9	58.2	84.2
k_1 (min^{-1})	0.0274	0.049	0.0302
R^2	0.859	0.981	0.963
PSO			
q_{cal}	61.7	69.9	66.7
$k_2 \times 10^{-3}$	1.16	1.11	2.32
R^2	0.998	0.998	0.999
Intraparticle diffusion			
k_p	6.24	7.21	9.26
C	2.33	2.58	18.8
R^2	0.9454	0.976	0.959

Therefore, the Weber–Morris intraparticle diffusion model was used to further clarify the adsorption mechanism. The model is based on Fick's second law of diffusion and is given by the following Eq. (8) [51]:

$$Q_t = k_{id} t^{1/2} + C \quad (8)$$

where C is related to the boundary layer effect and k_{id} is the intraparticle diffusion rate constant (mg/g $min^{1/2}$). The values of C and k_{id} can be evaluated from the intercept and slope of q_t vs. $t^{1/2}$, as shown in Fig. 12.

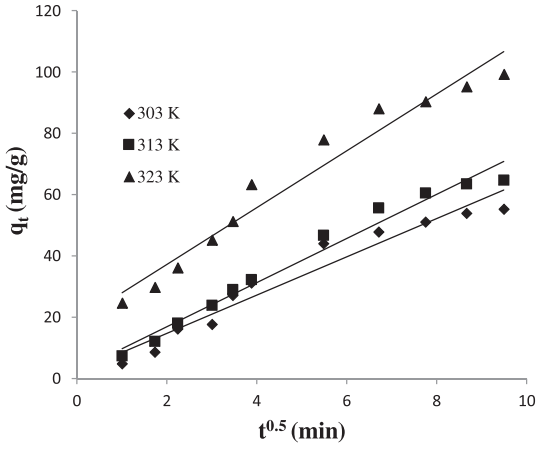

Fig. 12. The intraparticle diffusion plots for the adsorption of MB onto SAC at variable temperatures.

According to this model, a non-zero C value (Table 4) implies that there is an initial boundary resistance layer, where a larger C value indicates a greater boundary layer effect [52]. The C parameter reconfirms that the intraparticle diffusion effect is not the only rate-limiting step, but also other kinetic models may account for the rate of adsorption, and various processes may contribute simultaneously [22]. Table 4 shows the R^2 values for the intraparticle diffusion model provide a better fit than the PSO kinetic model. Similar observations have been reported in a previous study for the adsorption properties of the AC from H_2SO_4-treated bagasse [4], *Euphorbia Rigida* [22] and sunflower oil cake [25]. In this study, the PSO rate constants for MB onto SAC show an increase beyond twofold as the temperature increases from 303 to 323 K.

3.5. Adsorption thermodynamics

The thermodynamic adsorption parameters of MB onto SAC were computed from the experimental data obtained at 303, 313 and 323 K. The standard change in Gibbs energy (ΔG°), enthalpy (ΔH°) and entropy (ΔS°) were calculated using the following Eqs. (9)–(11) [53]:

$$k_d = \frac{q_e}{C_e} \tag{9}$$

$$\Delta G^\circ = -RT \ln k_d \tag{10}$$

$$\ln k_d = \frac{\Delta S^\circ}{R} - \frac{\Delta H^\circ}{RT} \tag{11}$$

where k_d is the distribution coefficient, q_e is the concentration of MB adsorbed on SAC at equilibrium (mg/L), C_e is the equilibrium concentration of MB in the liquid phase (mg/L), R is the universal gas constant (8.314 J/mol K) and T is the absolute temperature (K). The values of ΔH° and ΔS° were calculated from the slope and intercept of van't Hoff plots of ln k_d vs. $1/T$, respectively. The thermodynamic parameters are listed in Table 5. In general, the value for ΔG°, energy for physisorption ranges from −20 to 0 kJ/mol, the physisorption together with chemisorption falls at the range of −20 to −80 kJ/mol and chemisorption is more negative in magnitude with a range of −80 to −400 kJ/mol [54]. During the adsorption process, the negative values of ΔG° for the experimental range of temperatures (as recorded in Table 5) indicate spontaneous and favourable methylene blue adsorption onto the surface of SAC. The enthalpy for physisorption is generally below 0 kJ/mol, while for the chemisorption is a more negative range (80–420 kJ/mol) of values [55]. Therefore, the positive change for enthalpy of adsorption (ΔH° = +29.82 kJ/mol) obtained in this study for the SAC–MB system indicates that the adsorption process is mildly endothermic but the adsorption process follows a physisorption mechanism. The positive entropy change (ΔS°) value of 129.18 J/mol K corresponds to an increase in the degree of freedom of the adsorbed species due to adsorbate disorder and/or loss of water upon binding of MB to the SAC surface.

Table 5
Thermodynamic parameters values for the adsorption of MB onto SAC

	Thermodynamic parameters				
Temperature (K)	k_d	ΔG° (kJ/mol)	ΔH° (kJ/mol)	ΔS° (J/mol K)	E_a (kJ/mol)
303	43.7	−9.51	29.8	129.2	29.7
313	50.2	−10.2			
323	91.3	−12.1			

3.6. Activation energy of adsorption

The Arrhenius relationship was used to evaluate the activation energy of adsorption representing the minimum energy that reactants must possess for the reaction to proceed.

$$\ln k_2 = \ln A - \frac{E_a}{R} \cdot \frac{1}{T} \quad (12)$$

where k_2 is the rate constant obtained from the PSO model, E_a is the Arrhenius activation energy of adsorption, A is the Arrhenius pre-exponential factor, R is the gas constant, and is equal to 8.314 J/ mol K, and T is the temperature. According to the van't Hoff plots given by Eq. (12), the linear dependence yields a straight line (not shown) with slope ($-E_a/R$) that provides an estimate of E_a. The magnitude of activation energy gives an idea of a type of adsorption, which is either physical or chemical in nature. The value of E_a ranges over a narrow range (5–40 kJ/mol) that corresponds to a physisorption mechanism. A higher range of values is not observed (40–800 kJ/mol) for E_a which suggests that a chemisorption mechanism can be ruled out [56], according to the activation energy (29.7 kJ/mol) obtained. This physisorption mechanism of methylene blue onto the SAC surface is in agreement with thermodynamic results in Table 5.

4. Conclusions

The research work clearly shows that AC prepared from coconut leaves with activation by H_2SO_4 provides a low-cost adsorbent for the removal of a basic dye (methylene blue) from aqueous solutions. The adsorption properties under dynamic conditions are described by the pseudo-second-order model, while adsorption results at equilibrium are described by the Langmuir model. The maximum adsorption capacities (mg/g) of 126.9, 137.0 and 149.3 mg/g were obtained at 303, 313 and 323 K, respectively. The thermodynamic parameters indicate that the adsorption process is endothermic in nature and driven by entropy to yield a spontaneous adsorption process.

Acknowledgements

The authors would like to thank the Ministry of Education, Malaysia, for funding this research work under the Research Acculturation Grant Scheme (600-RMI/RAGS 5/3(18/2014). The authors also thank the Research Management Institute (RMI) and the Universiti Teknologi MARA for supporting the research work. The authors would like to thank Prof. Dr Bassim H. Hameed, School of Chemical Engineering, Universiti Sains Malaysia, for his fruitful discussions.

References

[1] F. Kaouah, S. Boumaza, T. Berrama, M. Trari, Z. Bendjama, Preparation and characterization of activated carbon from wild olive cores (oleaster) by H_3PO_4 for the removal of Basic Red 46, J. Cleaner Prod. 54 (2013) 296–306.
[2] T.B. Pushpa, J. Vijayaraghavan, S.J.S. Basha, V. Sekaran, K. Vijayaraghavan, J. Jegan, Investigation on removal of malachite green using EM based compost as adsorbent, Ecotoxicol. Environ. Saf. 118 (2015) 177–182.
[3] I.A.W. Tan, A.L. Ahmad, B.H. Hameed, Enhancement of basic dye adsorption uptake from aqueous solutions using chemically modified oil palm shell activated carbon, Colloids Surf. A 318 (2008) 88–96.
[4] L.W. Low, T.T. Teng, A. Ahmad, N. Morad, Y.S. Wong, A novel pretreatment method of lignocellulosic material as adsorbent and kinetic study of dye waste adsorption, Water Air and Soil Pollut. 218 (2011) 293–306.
[5] S. Senthilkumaar, P.R. Varadarajan, K. Porkodi, C.V. Subbhuraam, Adsorption of methylene blue onto jute fiber carbon: Kinetics and equilibrium studies, J. Colloid Interface Sci. 284 (2005) 78–82.
[6] A.H. Jawad, R.A. Rashid, R.M.A. Mahmuod, M.A.M. Ishak, N.N. Kasima, K. Ismail, Adsorption of methylene blue onto coconut (*Cocos nucifera*) leaf: Optimization, isotherm and kinetic studies, Desalin. Water Treat. (2015) 1–15, doi: 10.1080/19443994.2015.1026282.
[7] A.R. Khataee, A. Movafeghi, S. Torbati, S.Y. SalehiLisar, M. Zarei, Phytoremediation potential of duckweed (Lemna minor L.) in degradation of C.I. Acid Blue 92: Artificial neural network modeling, Ecotoxicol. Environ. Saf. 80 (2012) 291–298.
[8] L. Fan, Y. Zhou, W. Yang, G. Chen, F. Yang, Electrochemical degradation of aqueous solution of Amaranth azo dye on ACF under potentiostatic model, Dyes Pigm. 76 (2008) 440–446.
[9] J.S. Wu, C.H. Liu, K.H. Chu, S.Y. Suen, Removal of cationic dye methyl violet 2B from water by cation exchange membranes, J. Membr. Sci. 309 (2008) 239–245.
[10] Y.S. Woo, M. Rafatullah, A.F.M. Al-Karkhi, T.T. Tow, Removal of Terasil Red R dye by using Fenton oxidation: A statistical analysis, Desalin. Water Treat. 52 (2014) 4583–4591.
[11] A.H. Jawad, A.F.M. Alkarkhi, N.S.A. Mubarak, Photocatalytic decolorization of methylene blue by an immobilized TiO_2 film under visible light irradiation: Optimization using response surface methodology (RSM), Desalin. Water Treat. 56 (2015) 161–172.
[12] A.H. Jawad, N.S.A. Mubarak, M.A.M. Ishak, K. Ismail, W.I. Nawawi, Kinetics of photocatalytic decolourization of cationic dye using porous TiO_2 film, J. Taibah Univ. Sci. (2015) 1–11, doi: 10.1016/j.jtusci.2015.03.007.
[13] P. Canizares, F. Martınez, C. Jimenez, J. Lobato, M.A. Rodrigo, Coagulation and electrocoagulation of wastes

polluted with dyes, Environ. Sci. Technol. 40 (2006) 6418–6424.
[14] M.J. Ahmed, S.K. Dhedan, Equilibrium isotherms and kinetics modelling of methylene blue adsorption on agricultural wastes-based activated carbons, Fluid Phase Equilib. 317 (2012) 9–14.
[15] M.A. Kumar, V.V. Kumar, R. Ponnusamy, F.P. Daniel, M. Seenuvasan, D. Anuradha, S. Sivanesane, Concomitant mineralization and detoxification of acid red 88 by an indigenous acclimated mixed culture, Environ. Prog. Sustainable Energy 34 (2015) 1455–1466.
[16] T. Vidhyadevi, A. Murugesan, S.S. Kalaivani, M.A. Kumar, K.V.T. Ravi, L. Ravikumar, C.D. Anuradha, S. Sivanesan, Optimization of the process parameters for the removal of reactive yellow dye by the low cost Setaria verticillata carbon using response surface methodology: Thermodynamic, kinetic, and equilibrium studies, Environ. Prog. Sustainable Energy 33 (2014) 855–865.
[17] S. Karthikeyan, M.A. Kumar, P. Maharaja, T. Partheeban, J. Sridevi, G. Sekaran, Process optimization for the treatment of pharmaceutical wastewater catalyzed by poly sulpha sponge, J. Taiwan Instit. Chem. Eng. 45 (2014) 1739–1747.
[18] A. Sivapragasam, in: Paper Presented at the Second International Plantation Industry Conference and Exhibition (IPICEX2008), Shah Alam, Malaysia, 18–21 November, 2008, pp. 1–9
[19] I. Okman, S. Karagöz, T. Tay, M. Erdem, Activated carbons from grape seeds by chemical activation with potassium carbonate and potassium hydroxide, Appl. Surf. Sci. 293 (2014) 138–142.
[20] M. Hejazifar, S. Azizian, H. Sarikhani, Q. Li, D. Zhao, Microwave assisted preparation of efficient activated carbon from *grapevine rhytidome* for the removal of methyl violet from aqueous solution, J. Anal. Appl. Pyrolysis 92 (2011) 258–266.
[21] A. Gürses, Ç. Doğar, S.M. Karaca, M. Açikyildiz, R. Bayrak, Production of granular activated carbon from waste Rosa canina sp. seeds and its adsorption characteristics for dye, J. Hazard. Mater. 131 (2006) 254–259.
[22] Ö. Gerçel, A. Özcan, A.S. Özcan, H.F. Gerçel, Preparation of activated carbon from a renewable bio-plant of Euphorbia rigida by H_2SO_4 activation and its adsorption behavior in aqueous solutions, Appl. Surf. Sci. 253 (2007) 4843–4852.
[23] H. Hasar, Adsorption of nickel (II) from aqueous solution onto activated carbon prepared from almond husk, J. Hazard. Mater. 97 (2003) 49–57.
[24] H. Lata, V.K. Garg, R.K. Gupta, Removal of a basic dye from aqueous solution by adsorption using *Parthenium hysterophorus*: An agricultural waste, Dyes Pigm. 74 (2007) 653–658.
[25] S. Karagöz, T. Tay, S. Ucar, M. Erdem, Activated carbons from waste biomass by sulfuric acid activation and their use on methylene blue adsorption, Bioresour. Technol. 99 (2008) 6214–6222.
[26] B. Royer, N.F. Cardoso, E.C. Lima, J.C.P. Vaghetti, R.C. Veses, Applications of Brazalin pine-fruit shell in natural and carbonized forms as adsorbents to removal of methylene blue from aqueous solutions: Kinetics and equilibrium study, J. Hazard. Mater. 164 (2009) 1213–1222.
[27] Y.S. Ho, R. Malaryvizhi, N. Sulochana, Equilibrium isotherm studies of methylene blue adsorption onto activated carbon prepared from *Delonix regia* pods, J. Environ. Prot. Sci. 3(1) (2009) 1–6.
[28] N. Sharma, D.P. Tiwari, S.K. Singh, The efficiency appraisal for removal of malachite green by potato peel and neem bark: Isotherm and kinetic studies, Int. J. Chem. Environ. Eng. 5 (2014) 83–88.
[29] V.K. Garg, R. Kumar, R. Gupta, Removal of malachite green dye from aqueous solution by adsorption using agro-industry waste: A case study of Prosopis cineraria, Dyes Pigm. 62 (2004) 1–10.
[30] M. Auta, B.H. Hameed, Optimized waste tea activated carbon for adsorption of Methylene Blue and Acid Blue 29 dyes using response surface methodology, Chem. Eng. J. 175 (2011) 233–243.
[31] M. Ahmedna, W.E. Marshall, R.M. Rao, S.J. Clarke, Use of filtration and buffers in raw sugar colour measurements, J. Sci. Food Agric. 75 (1997) 109–116.
[32] F.A. Adekola, H.I. Adegoke, Adsorption of blue-dye on activated carbons produced from rice husk, coconut shell and coconut coir pith, Ife J. Sci. 7 (2005) 151–157.
[33] ASTM Standard, Standard test method for total ash content of activated carbon, ASTM International West Conshohocken, 2011, PA, doi: 10.1520/D2866-11.
[34] Lubrizol standard test method, Iodine value, test procedure AATM 1112-01, 16 October, 2006. Available from: <https://www.google.com/url?sa=t&rct=j&q=&esrc=s&source=web&cd=2&cad=rja&uact=8&ved=0ahUKEwiLx-eysMzKAhUGCY4KHV2PAi0QFggnMAE&url=https%3A%2F%2Fwww.lubrizol.com%2FWorkArea%2Flinkit.aspx%3FLinkIdentifier%3Did%26ItemID%3D5216&usg=AFQjCNFDJcbCej0Sb5Nlt2XzqMTQ_5-4xQ&bvm=bv.112766941,d.c2E>.
[35] L. Kong, L. Gong, L. Wang, Removal of methylene blue from wastewater using fallen leaves as an adsorbent, Desalin. Water Treat. 53 (2015) 2489–2500.
[36] R. Gnanasambandam, A. Protor, Determination of pectin degree of esterification by diffuse reflectance Fourier transforms infrared spectroscopy, Food Chem. 68 (2000) 327–332.
[37] M. Benadjemia, L. Millière, L. Reinert, N. Benderdouche, L. Duclaux, Preparation, characterization and Methylene Blue adsorption of phosphoric acid activated carbons from globe artichoke leaves, Fuel Process. Technol. 92 (2011) 1203–1212.
[38] G.E. Nascimento, M.M.M.B. Duarte, N.F. Campos, O.R.S. Rocha, V.L. Silva, Adsorption of azo dyes using peanut hull and orange peel: A comparative study, Environ. Technol. 35 (2014) 1436–1453.
[39] S. Liang, X. Guo, N. Feng, Q. Tian, Isotherms, kinetics, and thermodynamic studies of adsorption of Cu^{2+} from aqueous solutions by Mg^{2+}/K^{+} type orange peel adsorbent, J. Hazard. Mater. 174 (2010) 756–762.
[40] S. Chakraborty, S. Chowdhury, P.D. Saha, Adsorption of Crystal Violet from aqueous solution onto NaOH-modified rice husk, Carbohydr. Polym. 86 (2011) 1533–1541.
[41] W.T. Tsai, C.W. Lai, K.J. Hsien, Adsorption kinetics of herbicide paraquat from aqueous solution onto activated bleaching earth, Chemosphere 55 (2004) 829–837.

[42] I. Langmuir, The adsorption of gases on plane surfaces of glass, mica and platinum, J. Am. Chem. Soc. 40(9) (1918) 1361–1403.
[43] T.W. Weber, R.K. Chakkravorti, Pore and solid diffusion models for fixed bed adsorbers, AlChE J. 20(1974) (1974) 228.
[44] H.M.F. Freundlich, Over the adsorption in solution, J. Phys. Chem. 57 (1906) 385–470.
[45] K.R. Hall, L.C. Eagleton, A. Acrivos, T. Vermeulen, Pore- and solid diffusion kinetics in fixed-bed biosorption under constant-pattern conditions, Ind. Eng. Chem. Fundam. 5 (1966) 212–223.
[46] K. Fytianos, E. Voudrias, E. Kokkalis, Sorption–desorption behavior of 2, 4-dichloriphenol by marine sediments, Chemosphere 40 (2000) 3–6.
[47] D. Pathania, S. Sharma, P. Singh, Removal of methylene blue by adsorption onto activated carbon developed from *Ficus carica* bast, Arab. J. Chem. (2013) 1–7. Available from: <http://doi.org/10.1016/j.arabjc.2013.04.021>.
[48] K. Kadirvelu, M. Kavipriya, C. Karthika, M. Radhika, N. Vennilamani, S. Pattabhi, Utilization of various agricultural wastes for activated carbon preparation and application for the removal of dyes and metal ions from aqueous solutions, Bioresour. Technol. 87 (2003) 129–132.
[49] S. Lagergren, Zur theorie der sogenannten adsorption geloster stoffe, K. Sven. Vetenskapsakad. Handl. 24 (1898) 1–39.
[50] Y.S. Ho, G. McKay, Sorption of dye from aqueous solution by peat, Chem. Eng. J. 70 (1998) 115–124.
[51] W.J. Weber, J.C. Morris, Kinetics of adsorption on carbon from solution, J. Sanit. Eng. Divi. 89 (1963) 31–60.
[52] D. Kavitha, C. Namasivayam, Experimental and kinetic studies on methylene blue adsorption by coir pith carbon, Bioresour. Technol. 98 (2007) 14–21.
[53] G. Karaçetin, S. Sivrikaya, M. Imamoğlu, Adsorption of methylene blue from aqueous solutions by activated carbon prepared from hazelnut husk using zinc chloride, J. Anal. Appl. Pyrolysis 110 (2014) 270–276.
[54] M.J. Jaycock, G.D. Parfitt, Chemistry of Interfaces, Ellis Horwood Ltd., Onichester, 1981.
[55] K.E. Noll, V. Gounaris, W.S. Hou, Adsorption Technology for Air and Water Pollution Control, Lewis Publishers, Chelsea, MI, 1992, 21–22.
[56] H. Nollet, M. Roels, P. Lutgen, P.V. Meeren, W. Verstraete, Removal of PCBs from wastewater using fly ash, Chemosphere 53 (2003) 655–665.